

# Mechanics and Manipulation of Planar Elastic Kinematic Chains

Zoe McCarthy and Timothy Bretl

**Abstract**—In this paper, we study quasi-static manipulation of a planar kinematic chain with a fixed base in which each joint is a linearly-elastic torsional spring. The shape of this chain when in static equilibrium can be represented as the solution to a discrete-time optimal control problem, with boundary conditions that vary with the position and orientation of the last link. We prove that the set of all solutions to this problem is a smooth manifold that can be parameterized by a single chart. For manipulation planning, we show several advantages of working in this chart instead of in the space of boundary conditions, particularly in the context of a sampling-based planning algorithm. Examples are provided in simulation.

## I. INTRODUCTION

Consider a serial kinematic chain that moves in a planar workspace and that has a fixed base. Assume that each joint in this chain is a linearly-elastic torsional spring and that the last link is held by a robotic gripper. The problem we address is to find a path of the gripper that causes the chain to move between given start and goal configurations while remaining in static equilibrium and avoiding collision. This problem is a simple example of quasi-static manipulation planning in which the object to be manipulated is deformable.

What makes this problem hard is the apparent lack of coordinates to describe equilibrium configurations—i.e., configurations of the chain that would be in static equilibrium if the last link were held fixed by the gripper. The set of all equilibrium configurations has lower dimension than the configuration space of the chain, so elements of this set cannot be found by rejection sampling. Also, there are a countable number of equilibrium configurations that correspond to a given placement of the gripper, none of which can be computed in closed form. For this reason, most of the literature on similar problems would suggest exploring the set of equilibrium configurations indirectly, by sampling placements of the gripper and using numerical simulation to find their effect on the chain. This approach was developed at length in the seminal work of Lamiroux and Kavraki [1], and was later applied by Moll and Kavraki [2] to manipulation of elastic “deformable linear objects” like flexible wire, which can be viewed as a continuous analog of the elastic kinematic chain we consider here. Our own work is really a direct extension of [2], where we look at a simpler finite-dimensional object (the chain) in order to develop the basis for an alternative approach.

Our contribution in this paper is to prove that the set of equilibrium configurations for an elastic kinematic chain

is, in fact, a smooth manifold that can be parameterized explicitly by a single chart. In other words, we will produce a finite set of coordinates that suffice to describe all possible configurations of the chain that can be achieved by quasi-static manipulation. The key idea is to express equilibrium configurations as local optima of a discrete-time optimal control problem. Rather than try to compute solutions to this problem for given boundary conditions, we ask what must be satisfied by solutions to this problem for *any* boundary conditions. The coordinates we need are provided by costates that arise in necessary and sufficient conditions for optimality. Manipulation planning becomes very easy if we work in the chart defined by these coordinates.

We are motivated in part by the wide variety of applications that require manipulation of deformable objects. Knot tying has been a particular focus of the robotics community because of its potential application to surgical suturing [3]–[8], but other applications of interest include cable routing [9], folding clothes [10]–[12], robotic origami [13], assembly of flexible circuit boards [14], surgical retraction of tissue [15], compliant parts handling [16]–[18], and the closely related fields of protein folding and geometric analysis of molecular motion [19]–[22]. The theory we develop in this paper may shed new light on some of these problems, but we acknowledge that much remains to be done before any of our work can be applied in practice.

We are also motivated by the interesting link, pointed out by Tanner [23], between manipulation of deformable objects and control of hyper-redundant [24] and continuum [25]–[29] robots. These robots typically have many more degrees of freedom than are required to accomplish a given task. One approach to kinematic redundancy resolution is to choose a cost function and to restrict motion to the set of configurations that are locally optimal with respect to this cost function [30]. The robot then becomes a “deformable object” that is controlled by specifying the position and orientation of its end-effector. Our results show that it may be possible to parameterize the resulting set of locally optimal configurations. The coordinates we provide are an alternative to working either in the task space [31], [32] or in the space of modal shapes derived from a heuristic choice of basis functions [33]. Similar ideas have been applied to dynamic redundancy resolution [34], [35], and are related to the concept of operational space control [36].

Our main result appears in Section II, where we characterize the set of equilibrium configurations for a planar elastic kinematic chain. We apply this result to manipulation planning in Section III. We conclude with a brief discussion of future work in Section IV, leaving proofs to the Appendix.

Z. McCarthy is with the Department of Electrical and Computer Engineering and T. Bretl is with the Department of Aerospace Engineering, University of Illinois at Urbana-Champaign, Urbana, IL, 61801, USA {mccarth4, tbretl}@illinois.edu

## II. MECHANICS

In Section II-A, we fix notation and express equilibrium configurations of an elastic kinematic chain as local optima of a discrete-time optimal control problem (2). In Section II-B, we show that the set of configurations satisfying necessary conditions for local optimality is a smooth 3-manifold (Theorem 2). In Section II-C, we show that the set of configurations satisfying sufficient conditions for local optimality is an open subset of this manifold, and we provide an algorithm to test membership in this subset (Theorem 4).

### A. Model

The kinematic chain in Fig. 1 moves in a planar workspace  $\mathcal{W} = \mathbb{R}^2$ . It has  $n$  revolute joints, where we assume  $n > 3$ . We index joints by  $i \in \{0, \dots, n-1\}$ . The angle of each joint  $i$  is  $u(i) \in \mathbb{R}$ . We denote the entire sequence of joint angles by the function  $u: \{0, \dots, n-1\} \rightarrow \mathbb{R}$ . We call the space of all possible  $u$  the joint space and identify it in the obvious way with  $\mathcal{Q} = \mathbb{R}^n$ . The chain has  $n+1$  rigid links that we index by  $i = \{0, \dots, n\}$ . We attach a coordinate frame to each link  $1, \dots, n$  so that the axis of joint  $i-1$  passes through the origin of frame  $i$ . We attach a coordinate frame to link 0 so that the origin of frames 0 and 1 coincide. We describe the position and orientation of frame  $i$  relative to frame 0 by the homogenous transformation matrix

$$\begin{bmatrix} \cos x_3(i) & -\sin x_3(i) & x_1(i) \\ \sin x_3(i) & \cos x_3(i) & x_2(i) \\ 0 & 0 & 1 \end{bmatrix} \in SE(2)$$

for some  $x(i) \in \mathbb{R}^3$ . Henceforth, we refer only to  $x(i)$  and not to the element of  $SE(2)$  to which  $x(i)$  corresponds. This choice is for convenience and will cause no problems. It can be viewed as working in the chart  $\mathbb{R}^2 \times (x_3(i) - \pi, x_3(i) + \pi)$ . We call  $x(i)$  the state and call  $\mathcal{X} = \mathbb{R}^3$  the state space. We specify  $x(i)$  recursively with the finite difference equation

$$x(i+1) = x(i) + \begin{bmatrix} r_i \cos x_3(i) \\ r_i \sin x_3(i) \\ u(i) \end{bmatrix} \quad (1)$$

for  $i \in \{0, \dots, n-1\}$ , where for convenience we choose

$$r_i = \begin{cases} 0 & \text{if } i = 0, \\ (n-1)^{-1} & \text{otherwise} \end{cases}$$

so that the total length is 1. We denote the state trajectory by  $x: \{0, \dots, n\} \rightarrow \mathcal{X}$ . Each end of the kinematic chain is held by a robotic gripper. We ignore the structure of these grippers, and simply assume that they fix arbitrary values of  $x(0)$  and  $x(n)$ . We further assume, without loss of generality, that  $x(0) = 0$ . We call the space of all possible  $x(n)$  the task space and denote it by  $\mathcal{B} \subset \mathbb{R}^3$ . Again, the reader should think of each  $b \in \mathcal{B}$  as belonging to a chart of  $SE(2)$ .

Finally, we assume that each joint  $i$  in the kinematic chain is a linearly-elastic torsional spring with unit modulus and so has potential energy  $u(i)^2/2$ . For fixed endpoints, the chain will remain motionless only if its shape locally minimizes the

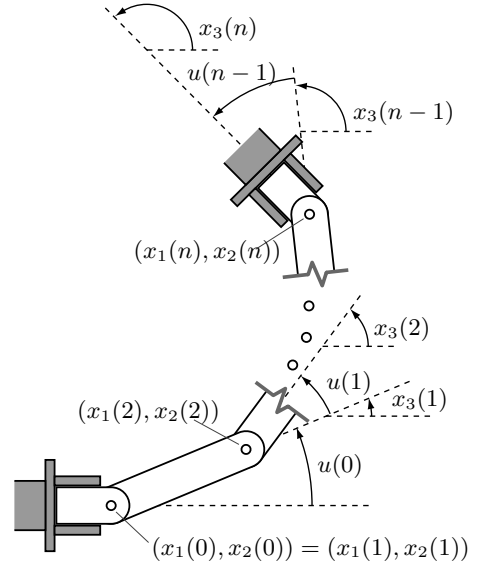


Fig. 1. A planar kinematic chain with  $n$  joints and  $n+1$  rigid links that is held at each end by a robotic gripper. Each joint is a linearly elastic torsional spring. For a fixed position and orientation of each gripper, the chain relaxes to a shape that locally minimizes the energy in all  $n$  joints.

total energy in all  $n$  joints. In particular, we say that  $(u, x)$  is in static equilibrium if it is a locally optimal solution to

$$\begin{aligned} & \underset{\substack{u \in \mathcal{Q} \\ x(0), \dots, x(n) \in \mathcal{X}}}{\text{minimize}} && \frac{1}{2} \sum_{i=0}^{n-1} u(i)^2 \\ & \text{subject to} && x(i+1) = x(i) + \begin{bmatrix} r_i \cos x_3(i) \\ r_i \sin x_3(i) \\ u(i) \end{bmatrix} \quad (2) \\ & && \text{for all } i \in \{0, \dots, n-1\} \\ & && x(0) = 0 \\ & && x(n) = b \end{aligned}$$

for some  $b \in \mathcal{B}$ .

### B. Necessary Conditions for Static Equilibrium

The following theorem is an application of first-order necessary conditions for equality-constrained minimization to the problem (2), similar to [37, Chap. 2.6]:

*Theorem 1:* If  $(u, x)$  is both regular and a local optimum of (2), then there exists a costate trajectory

$$p: \{0, \dots, n\} \rightarrow \mathbb{R}^3$$

that satisfies

$$p(i)^T = \nabla_{x(i)} H(x(i), p(i+1), u(i)) \quad (3)$$

$$0 = \nabla_{u(i)} H(x(i), p(i+1), u(i)) \quad (4)$$

for all  $i \in \{0, \dots, n-1\}$ , where

$$\begin{aligned} H(x(i), p(i+1), u(i)) &= \frac{1}{2} u(i)^2 \\ &+ p_1(i+1) (x_1(i) + r_i \cos x_3(i)) \\ &+ p_2(i+1) (x_2(i) + r_i \sin x_3(i)) \\ &+ p_3(i+1) (x_3(i) + u(i)) \end{aligned}$$

is the Hamiltonian function.

*Proof:* See [38, Chap. 11.3]. ■

Theorem 1 provides a set of candidates for local optimality of (2), which we will proceed to characterize. Let  $\mathcal{C} \subset \mathbb{R}^n \times \mathbb{R}^{3(n+1)}$  be the set of all regular  $(u, x)$  for which there exists  $p$  satisfying (3)-(4). We will show that  $\mathcal{C}$  is a smooth 3-manifold. In particular, equations (3)-(4) require that

$$\begin{aligned} p(i)^T &= p(i+1)^T J_i \\ u(i) &= -p(i+1)^T e_3 \end{aligned}$$

for  $i \in \{0, \dots, n-1\}$ , where

$$J_i = \begin{bmatrix} 1 & 0 & -r_i \sin x_3(i) \\ 0 & 1 & r_i \cos x_3(i) \\ 0 & 0 & 1 \end{bmatrix} \quad \text{and} \quad e_3 = \begin{bmatrix} 0 \\ 0 \\ 1 \end{bmatrix}.$$

The inverse  $J_i^{-1}$  exists everywhere. Hence,  $(u, x)$  and  $p$  are related by the finite difference equations

$$\begin{aligned} u(i) &= -p(i)^T J_i^{-1} e_3 \\ x(i+1) &= x(i) + \begin{bmatrix} r_i \cos x_3(i) \\ r_i \sin x_3(i) \\ u(i) \end{bmatrix} \\ p(i+1) &= J_i^{-T} p(i) \end{aligned} \quad (5)$$

for  $i \in \{0, \dots, n-1\}$ . Recalling that  $x(0) = 0$ , we see that (5) is completely defined by the choice of  $p(0)$ . For  $a \in \mathbb{R}^3$ , let  $p(0) = a$  and compute  $(u, x)$  and  $p$  according to (5). Denote the resulting map by

$$\phi(a) = (u, x) \quad (6)$$

$$\rho(a) = p. \quad (7)$$

Define

$$\mathcal{A} = \left\{ a \in \mathbb{R}^3 : \begin{bmatrix} a_2 \\ a_3 \end{bmatrix} \notin \mathcal{S} \right\},$$

where

$$\mathcal{S} = \left\{ \begin{bmatrix} k(n-1)\pi \\ l\pi \end{bmatrix} \in \mathbb{R}^2 : k, l \in \mathbb{Z} \right\}$$

is exactly the set of points that map to singularities of the chain under  $\phi$  (see Lemma 5, Appendix II). We show in Appendix II that  $\phi: \mathcal{A} \rightarrow \mathcal{C}$  is a homeomorphism, and draw the following conclusion:

*Theorem 2:*  $\mathcal{C}$  is a smooth 3-manifold with smooth structure determined by an atlas with the single chart  $(\mathcal{C}, \phi^{-1})$ .

*Proof:* Since  $\phi$  is a homeomorphism by Lemma 6 (Appendix II) and  $\mathcal{A} \subset \mathbb{R}^3$  is open, then  $(\mathcal{C}, \phi^{-1})$  is a chart whose domain covers  $\mathcal{C}$ . Our result is an immediate consequence of Lemma 1 (Appendix I). ■

As a corollary, we know that  $\mathcal{A}$  is also a smooth 3-manifold and that  $\phi: \mathcal{A} \rightarrow \mathcal{C}$  is, in fact, a diffeomorphism.

### C. Sufficient Conditions for Static Equilibrium

Given  $(u, x) = \phi(a)$  and  $p = \rho(a)$  for  $a \in \mathcal{A}$ , we compute

$$\begin{aligned} \nabla_{u(i)u(i)}^2 H(x(i), p(i+1), u(i)) &= 1 \\ \nabla_{u(i)x(i)}^2 H(x(i), p(i+1), u(i)) &= [0 \quad 0 \quad 0] \\ \nabla_{x(i)x(i)}^2 H(x(i), p(i+1), u(i)) &= Q_i \end{aligned}$$

### DISCRETEISSTABLE(a)

Given  $a \in \mathcal{A}$ , do the following:

- Compute  $(u, x) = \phi(a)$  and  $p = \rho(a)$ .
- Compute

$$\begin{aligned} A &= \begin{bmatrix} e_3 & 0 & 0 & 0 & -I & 0 & 0 \\ 0 & e_3 & 0 & 0 & J_{n-3} & -I & 0 \\ 0 & 0 & e_3 & 0 & 0 & J_{n-2} & -I \\ 0 & 0 & 0 & e_3 & 0 & 0 & J_{n-1} \end{bmatrix} \\ B &= [-J_{n-4} \quad 0 \quad 0 \quad 0]^T \\ M &= \begin{bmatrix} I & 0 & 0 & 0 \\ 0 & Q_{n-3} & 0 & 0 \\ 0 & 0 & Q_{n-2} & 0 \\ 0 & 0 & 0 & Q_{n-1} \end{bmatrix}, \end{aligned}$$

and find a basis  $N$  for the null space of  $A$ . If

$$N^T M N > 0$$

then take

$$A^\dagger = A^T (A A^T)^{-1}$$

$$K = (N^T M N)^{-1} N^T M$$

$$P_{n-4} = (A^\dagger B)^T (I - N K)^T M (I - N K) (A^\dagger B),$$

otherwise return FALSE.

- For each  $i \in \{n-5, \dots, 0\}$ , if

$$s_{i+1} = 1 + e_3^T P_{i+1} e_3 > 0$$

then take

$$P_i = Q_i + J_i^T (P_{i+1} - P_{i+1} e_3 s_{i+1}^{-1} e_3^T P_{i+1}) J_i,$$

otherwise return FALSE.

Return TRUE.

Fig. 2. An algorithm that checks the membership of  $a$  in  $\mathcal{A}_{\text{stable}} \subset \mathcal{A}$ .

for  $i \in \{0, \dots, n-1\}$ , where

$$Q_i = \begin{bmatrix} 0 & 0 & 0 \\ 0 & 0 & 0 \\ 0 & 0 & -r_i (a_1 \cos x_3(i) + a_2 \sin x_3(i)) \end{bmatrix}.$$

Based on this result, the following theorem is an application of second-order sufficiency conditions for equality-constrained minimization, similar to [37, Chap 2.6]:

*Theorem 3:* Let  $(u, x) = \phi(a)$  and  $p = \rho(a)$  for  $a \in \mathcal{A}$ . If  $(\delta u, \delta x) = (0, 0)$  is the unique solution to

$$\begin{aligned} \text{minimize}_{\delta u \in \mathcal{Q}} & \frac{1}{2} \sum_{i=0}^{n-1} (\delta x(i)^T Q_i \delta x(i) + \delta u(i)^2) \\ \text{subject to} & \delta x(i+1) = J_i \delta x(i) + e_3 \delta u(i) \\ & \text{for all } i \in \{0, \dots, n-1\} \\ & \delta x(0) = 0 \\ & \delta x(n) = 0, \end{aligned} \quad (8)$$

then  $(u, x)$  is a local optimum of (2) for  $b = x(n)$ .

*Proof:* See [38, Chap. 11.5]. ■

Theorem 3 allows us to say which points  $a \in \mathcal{A}$  actually produce local optima  $\phi(a) \in \mathcal{C}$  of (2). In particular, let  $\mathcal{A}_{\text{stable}} \subset \mathcal{A}$  be the set of all  $a$  for which  $(\delta u, \delta x) = (0, 0)$  is the unique solution to (8), and let  $\mathcal{C}_{\text{stable}} = \phi(\mathcal{A}_{\text{stable}}) \subset \mathcal{C}$ . The following result establishes correctness of DISCRETEISSTABLE (Fig. 2), which tests membership in  $\mathcal{A}_{\text{stable}}$ :

*Theorem 4:* The point  $a \in \mathcal{A}$  is an element of  $\mathcal{A}_{\text{stable}}$  if and only if DISCRETEISSTABLE( $a$ ) returns TRUE.

*Proof:* See Appendix III. ■

Another important consequence of membership in  $\mathcal{A}_{\text{stable}}$  is smooth local dependence of (2) on variation in  $b$ . Define

$$\mathcal{B}_{\text{stable}} = \{x(n) \in \mathcal{B} : (u, x) \in \mathcal{C}_{\text{stable}}\}$$

and let  $\beta: \mathcal{C} \rightarrow \mathcal{B}$  be the map taking  $(u, x)$  to  $x(n)$ . We note that  $\mathcal{A}_{\text{stable}}$  is open, hence that  $\phi|_{\mathcal{A}_{\text{stable}}}: \mathcal{A}_{\text{stable}} \rightarrow \mathcal{C}_{\text{stable}}$  is a diffeomorphism. The following theorem is then an application of sensitivity analysis to equality-constrained minimization, similar to [37, Chap. 6.10-6.11]:

*Theorem 5:* The map

$$\beta \circ \phi|_{\mathcal{A}_{\text{stable}}}: \mathcal{A}_{\text{stable}} \rightarrow \mathcal{B}_{\text{stable}}$$

is a local diffeomorphism.

*Proof:* See [38, Chap. 11.7]. ■

### III. MANIPULATION

#### A. Planning Algorithm

The results of Section II make it very clear how to do manipulation planning for the planar elastic kinematic chain in Fig. 1. Recall that we would like to find a path of the gripper that causes the chain to move between given start and goal configurations while remaining in static equilibrium. What makes this problem seem hard is the apparent lack of coordinates to describe equilibrium configurations. Section II gives us the coordinates that we need. In particular, we showed that any equilibrium configuration can be represented by a point in the open subset  $\mathcal{A}_{\text{stable}} \subset \mathcal{A} \subset \mathbb{R}^3$ . It is entirely correct to think of  $\mathcal{A}$  as the “configuration space” of the chain during quasi-static manipulation, and to think of  $\mathcal{A}_{\text{stable}}$  as the “free space.” Theorem 2 tells us how to map points in  $\mathcal{A}$  to configurations of the chain. Theorem 4 tells us how to test membership in  $\mathcal{A}_{\text{stable}}$ , i.e., it gives us a “collision checker.” And finally, Theorem 5 tells us that paths in  $\mathcal{A}_{\text{stable}}$  can be “implemented” by the robotic gripper, by establishing a well-defined map between differential changes in the shape of the chain (represented by  $\mathcal{A}_{\text{stable}}$ ) and in the placement of the gripper (represented by  $\mathcal{B}_{\text{stable}}$ ). So, at this point, there is very little left to say. We have expressed the manipulation planning problem for planar elastic kinematic chains as a standard motion planning problem in a configuration space of dimension 3, for which there are hundreds of possible solution approaches [39]–[41].

For the sake of completeness, we will describe how one might implement a sampling-based planning algorithm like PRM [42]. Sample points in  $\mathcal{A}$ , for example uniformly at random in the closed subset  $\{a \in \mathcal{A} : \|a\|_{\infty} \leq w\}$  for some  $w > 0$ . Keep points that are in  $\mathcal{A}_{\text{stable}}$ —i.e., points  $a \in \mathcal{A}$  for

which DISCRETEISSTABLE( $a$ ) returns TRUE—and add these points as nodes in the roadmap. Try to connect each pair of nodes  $a$  and  $a'$  with a straight-line path in  $\mathcal{A}$ , adding this path as an edge in the roadmap if it lies entirely in  $\mathcal{A}_{\text{stable}}$ . Two points  $a_{\text{start}}$  and  $a_{\text{goal}}$  in  $\mathcal{A}_{\text{stable}}$  are path-connected if they can be connected by a sequence of nodes and edges in the roadmap. This sequence is a continuous and piecewise-differentiable path  $\alpha: [0, 1] \rightarrow \mathcal{A}_{\text{stable}}$ , where  $\alpha(0) = a_{\text{start}}$  and  $\alpha(1) = a_{\text{goal}}$ . The manipulation plan is the path

$$\beta \circ \phi|_{\mathcal{A}_{\text{stable}}} \circ \alpha: [0, 1] \rightarrow \mathcal{B}_{\text{stable}},$$

also continuous and piecewise-differentiable, which can be implemented by the robotic gripper. Note that it is easy to include additional constraints, such as joint limits and self-collision, within this basic framework.

In considering the manipulation planning problem, it is important to remember that there is a diffeomorphism between  $\mathcal{A}$  and  $\mathcal{C}$  (Theorem 2) but only a local diffeomorphism between  $\mathcal{A}$  and  $\mathcal{B}$  (Theorem 5). A problem may be equivalently defined by  $a_{\text{start}}, a_{\text{goal}} \in \mathcal{A}$  or  $c_{\text{start}}, c_{\text{goal}} \in \mathcal{C}$ , but may not be defined by  $b_{\text{start}}, b_{\text{goal}} \in \mathcal{B}$ , since points in task space do not uniquely specify configurations of the chain.

#### B. Example

As a simple example of quasi-static manipulation, we consider a chain with only four joints (Fig. 3). If we restrict  $|u(i)| \leq \pi$ , then there are at most two inverse kinematic solutions for any given  $u(0)$ , so it is possible to visualize the energy landscape and to see the local minima. Figure 3, in particular, shows three different equilibrium configurations associated with the same boundary conditions. Each one corresponds to a local minimum of potential energy. Also shown are snapshots of quasi-static manipulation from  $\phi(a_{\text{start}})$  to  $\phi(a_{\text{goal}})$  for a particular choice of  $a_{\text{start}}$  and  $a_{\text{goal}}$ . The motion of the chain in this case corresponds to a straight-line path in  $\mathcal{A}_{\text{stable}}$ , as might have been generated by a sampling-based planner. In other words, it is implemented by moving the gripper along the path  $\beta \circ \phi|_{\mathcal{A}_{\text{stable}}} \circ \alpha: [0, 1] \rightarrow \mathcal{B}_{\text{stable}}$ , where

$$\alpha(t) = (1-t)a_{\text{start}} + ta_{\text{goal}}.$$

It is interesting to consider what would have happened if we had tried to plan a path from  $\phi(a_{\text{start}})$  to  $\phi(a_{\text{goal}})$  by working in the task space  $\mathcal{B}$  rather than in the space  $\mathcal{A}$  of equilibrium configurations. Clearly, the resulting plan cannot be represented by a straight line in  $\mathcal{B}$ . Indeed, we have

$$\beta \circ \phi|_{\mathcal{A}_{\text{stable}}} \circ \alpha(a_{\text{start}}) = \beta \circ \phi|_{\mathcal{A}_{\text{stable}}} \circ \alpha(a_{\text{goal}})$$

in this case, so a straight line in  $\mathcal{B}$  takes you nowhere. In the language of sampling-based planning [40]–[42], we say that  $\phi(a_{\text{goal}})$  is visible from  $\phi(a_{\text{start}})$  when using a straight-line local connection strategy in  $\mathcal{A}$ , but is not visible when using a straight-line local connection strategy in  $\mathcal{B}$ . Indeed, although we have not performed exhaustive experiments, anecdotally we can say that planning in  $\mathcal{A}$  often requires sampling only a handful of nodes (less than 10), while planning in  $\mathcal{B}$  often requires sampling many more. This result—however preliminary—is an indication that our approach may have a

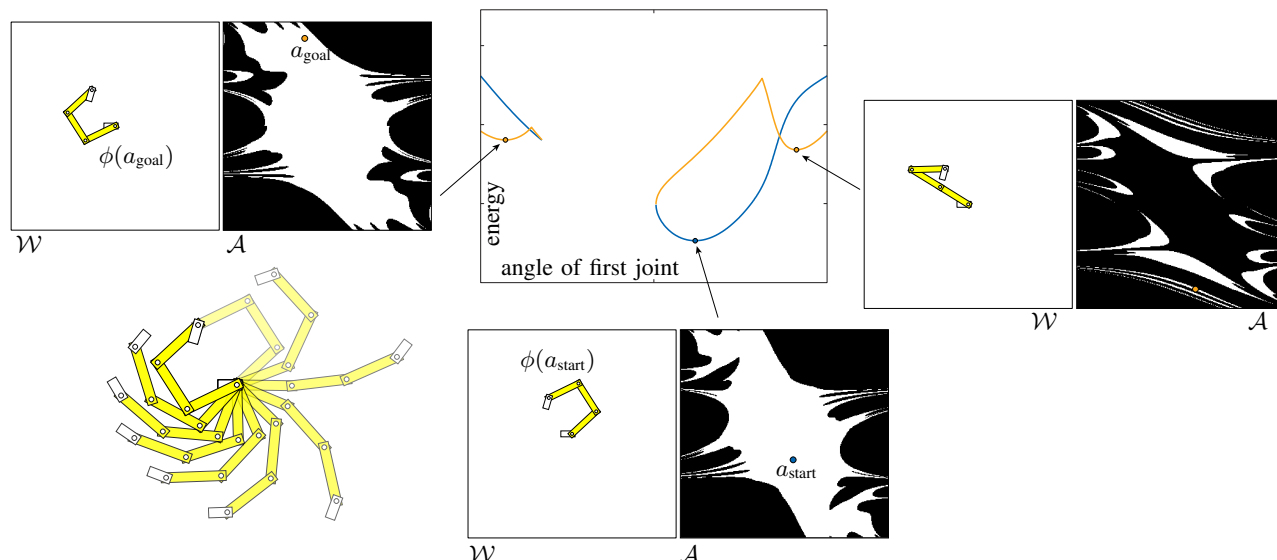


Fig. 3. Three equilibrium configurations of a four-joint elastic kinematic chain for fixed boundary conditions. Each one corresponds to a local minimum of potential energy, i.e., to a local optimum of (2). We show the point  $a \in \mathcal{A}$  and the configuration  $\phi(a) \in \mathcal{C}$  associated with each local minimum. We are showing only a slice of  $\mathcal{A}$  for fixed  $a_1$  in each case—the non-shaded part of this slice is in  $\mathcal{A}_{\text{stable}}$ . Snapshots of quasi-static manipulation from  $\phi(a_{\text{start}})$  to  $\phi(a_{\text{goal}})$ —given by a straight-line path from  $a_{\text{start}}$  to  $a_{\text{goal}}$ —are shown at lower left. In this example, the first link is held fixed and we imagine a robotic gripper is changing the position and orientation of the last link. The energy landscape of course varies along this path (see multimedia attachment).

number of practical advantages. For example, another clear advantage is that points in  $\mathcal{A}$  uniquely specify configurations of the chain, while the configuration specified by a point in  $\mathcal{B}$  depends on the path taken to get there.

Before closing, we note that the dimensionality of  $\mathcal{A}$  does not increase with the number of joints  $n$ . We find this result somewhat remarkable, because it means that the complexity of manipulation planning does not scale as it normally would. In particular, since the joint space of the chain—which is what we usually refer to as the configuration space—has dimension  $n$ , we would expect the complexity of planning to be at least exponential in  $n$ . In fact, since the dimension of  $\mathcal{A}$  remains constant (at 3), so does the complexity of planning. It is true that the execution of DISCRETEISSTABLE requires time that grows linearly in  $n$ , and that checking other constraints like self-collision would require similarly more time, but none of this is anywhere near exponential. In hindsight, we might have expected this result—since any quasi-static motion of the chain is caused by motion of the gripper, and since the configuration of the gripper lives in  $SE(2)$ , we conclude that the set of equilibrium configurations must at least locally have dimension three.

For other examples of quasi-static manipulation, in particular with large  $n$ , please see the multimedia attachment.

#### IV. CONCLUSION

In this paper, we looked at the problem of quasi-static manipulation planning for a kinematic chain with  $n$  joints that are linearly-elastic torsional springs. What has made this problem seem hard in the past is the apparent lack of coordinates to describe equilibrium configurations. Our contribution was to show that the set of equilibrium configurations in this case is, in fact, a smooth 3-manifold that can be parameterized globally by a single chart. This result allowed

us to treat manipulation planning like any other motion planning problem—it produced a “configuration space”  $\mathcal{A}$ , a “collision checker” to test membership in the part  $\mathcal{A}_{\text{stable}}$  of  $\mathcal{A}$  that corresponds to equilibrium configurations, and a diffeomorphism that allowed us to “implement” paths in  $\mathcal{A}_{\text{stable}}$  by paths of the gripper. We showed a simple example (for more, see the multimedia attachment) and briefly discussed several advantages of planning in  $\mathcal{A}$ . There are many opportunities for future work. For example, it is natural to extend what we have here to continuous models of flexible wire in both 2D and 3D workspaces, by application of Pontryagin’s maximum principle. It is also natural to consider an elastic kinematic chain (either discrete or continuous) with modulus of elasticity that varies along its length. This extension is an easy one, but gives rise to the much more interesting problem of “calibration”—how do you infer based on observation what is the modulus as a function of length? This problem can be cast as inverse optimal control and efficiently solved. We are looking at these and other topics now, and hope that they lead to results that can be applied in practice.

#### APPENDIX I SMOOTH MANIFOLDS

Here, we recall basic definitions and state two facts about smooth (i.e., differentiable) manifolds [43].

A *topological  $n$ -manifold*  $\mathcal{M}$  is a topological space that is Hausdorff, second countable, and locally Euclidean of dimension  $n$ . A *chart* on  $\mathcal{M}$  is a pair  $(\mathcal{U}, \alpha)$ , where  $\mathcal{U} \subset \mathcal{M}$  and  $\alpha(\mathcal{U}) \subset \mathbb{R}^n$  are both open and where  $\alpha: \mathcal{U} \rightarrow \alpha(\mathcal{U})$  is a homeomorphism. An *atlas* on  $\mathcal{M}$  is a collection of charts whose domain covers  $\mathcal{M}$ . Two charts  $(\mathcal{U}, \alpha)$  and  $(\mathcal{V}, \beta)$  on  $\mathcal{M}$  are *smoothly compatible* if either  $\mathcal{U}$  and  $\mathcal{V}$  are disjoint or the composition  $\beta \circ \alpha^{-1}$  is a diffeomorphism (i.e., is a smooth function between open subsets of  $\mathbb{R}^n$  that has a smooth

inverse, where by “smooth” we mean in the class  $C^\infty$ ). A *smooth atlas* is an atlas in which any two charts are smoothly compatible. A chart that is part of a smooth atlas is called a *smooth chart*. A smooth atlas is *maximal* if it is not contained in any other strictly larger smooth atlas. A maximal smooth atlas is called a *smooth structure*. A *smooth  $n$ -manifold* is a topological  $n$ -manifold equipped with a smooth structure. It can be shown that any smooth atlas is contained in a unique maximal smooth atlas, so to define a smooth  $n$ -manifold  $\mathcal{M}$  it suffices only to specify some smooth atlas on  $\mathcal{M}$ . A map  $f: \mathcal{M} \rightarrow \mathcal{N}$  between smooth manifolds  $\mathcal{M}$  and  $\mathcal{N}$  is a *smooth map* if for every  $p \in \mathcal{M}$ , there exist smooth charts  $(\mathcal{U}, \alpha)$  on  $\mathcal{M}$  and  $(\mathcal{V}, \beta)$  on  $\mathcal{N}$  such that

$$p \in \mathcal{U} \quad f(p) \in \mathcal{V} \quad f(\mathcal{U}) \subset \mathcal{V} \quad (9)$$

and  $\beta \circ f \circ \alpha^{-1}: \alpha(\mathcal{U}) \rightarrow \beta(\mathcal{V})$  is smooth. A *diffeomorphism* between smooth  $n$ -manifolds  $\mathcal{M}$  and  $\mathcal{N}$  is a smooth map  $f: \mathcal{M} \rightarrow \mathcal{N}$  that is bijective and that has a smooth inverse.

We require the following two results:

**Lemma 1:** If the topological  $n$ -manifold  $\mathcal{M}$  has an atlas consisting of the single chart  $(\mathcal{M}, \alpha)$ , then  $\mathcal{N} = \alpha(\mathcal{M})$  is a topological  $n$ -manifold with an atlas consisting of the single chart  $(\mathcal{N}, \text{id}_{\mathcal{N}})$ , where  $\text{id}_{\mathcal{N}}$  is the identity map. Furthermore, both  $\mathcal{M}$  and  $\mathcal{N}$  are smooth  $n$ -manifolds and  $\alpha: \mathcal{M} \rightarrow \mathcal{N}$  is a diffeomorphism.

*Proof:* Since  $(\mathcal{M}, \alpha)$  is chart, then  $\mathcal{N}$  is an open subset of  $\mathbb{R}^n$  and  $\alpha$  is a bijection. Hence, our first result is immediate and our second result requires only that both  $\alpha$  and  $\alpha^{-1}$  are smooth maps. For every  $p \in \mathcal{M}$ , the charts  $(\mathcal{M}, \alpha)$  and  $(\mathcal{N}, \text{id}_{\mathcal{N}})$  satisfy (9) and we have  $\text{id}_{\mathcal{N}} \circ \alpha \circ \alpha^{-1} = \text{id}_{\mathcal{N}}$ , so  $\alpha$  is a smooth map. For every  $q \in \mathcal{N}$ , the charts  $(\mathcal{N}, \text{id}_{\mathcal{N}})$  and  $(\mathcal{M}, \alpha)$  again satisfy (9) and we have  $\alpha \circ \alpha^{-1} \circ \text{id}_{\mathcal{N}} = \text{id}_{\mathcal{M}}$ , so  $\alpha^{-1}$  is also a smooth map, and our result follows. ■

**Lemma 2:** If the continuous bijection  $f: \mathcal{M} \rightarrow \mathcal{N}$  is a local homeomorphism, then  $\mathcal{M}$  and  $\mathcal{N}$  are homeomorphic.

*Proof:* We need only show that  $g = f^{-1}$  is continuous. This result holds if and only if each point of  $\mathcal{N}$  has a neighborhood on which the restriction of  $g$  to that neighborhood is continuous [44, Lemma 2.2]. Fix  $p \in \mathcal{N}$ . Since  $f$  is a local homeomorphism, there exists a neighborhood  $\mathcal{U}$  around  $g(p)$  such that  $f|_{\mathcal{U}}: \mathcal{U} \rightarrow f(\mathcal{U})$  is a homeomorphism. Let  $\mathcal{V} = f(\mathcal{U}) \subset \mathcal{N}$ . We know that  $\mathcal{V}$  is a neighborhood of  $p$  since  $\mathcal{U}$  is a neighborhood of  $g(p)$  and  $f|_{\mathcal{U}}$  is a homeomorphism. Since  $(f|_{\mathcal{U}})^{-1}$  is continuous and  $g|_{\mathcal{V}} = (f|_{\mathcal{U}})^{-1}$ , then our result follows. ■

## APPENDIX II

### PROOF THAT $\phi: \mathcal{A} \rightarrow \mathcal{C}$ IS A HOMEOMORPHISM

Our main result in this section is Lemma 6, which is necessary in the proof of Theorem 2 in Section II-B. We will first prove three supporting lemmas.

**Lemma 3:** If  $(u, x) = \phi(a)$  and  $p = \rho(a)$  for  $a \in \mathbb{R}^3$ , then

$$u(i) = -a_1 x_2(i+1) + a_2 x_1(i+1) - a_3$$

for  $i \in \{0, \dots, n-1\}$ .

*Proof:* From (5), we compute

$$\begin{aligned} p_1(i+1) &= p_1(i) \\ p_2(i+1) &= p_2(i) \\ p_3(i+1) &= p_1(i)(x_2(i+1) - x_2(i)) \\ &\quad - p_2(i)(x_1(i+1) - x_1(i)) + p_3(i) \end{aligned}$$

for  $i \in \{0, \dots, n-1\}$ . Since  $x(0) = 0$  and  $p(0) = a$ , it is equivalent that

$$\begin{aligned} p_1(i) &= a_1 \\ p_2(i) &= a_2 \\ p_3(i) &= a_1 x_2(i) - a_2 x_1(i) + a_3 \end{aligned}$$

for  $i \in \{0, \dots, n\}$ . We conclude that

$$\begin{aligned} u(i) &= -p(i+1)^T e_3 \\ &= -p_3(i+1) \\ &= -a_1 x_2(i+1) + a_2 x_1(i+1) - a_3, \end{aligned}$$

as desired. ■

**Lemma 4:** A point  $(u, x)$  is regular with respect to (2) if and only if

$$u(i) \notin \{k\pi: k \in \mathbb{Z}\}$$

for some  $i \in \{1, \dots, n-1\}$ .

*Proof:* The problem (2) has  $3n+6$  equality constraints. By definition, a point  $(u, x)$  is regular with respect to these constraints if the corresponding gradient vectors are linearly independent [38]. By direct computation, it is equivalent that

$$\begin{bmatrix} 0 & 0 & \dots & 0 & 0 & -I & 0 & \dots & 0 & 0 \\ e_3 & 0 & \dots & 0 & 0 & J_0 & -I & \dots & 0 & 0 \\ 0 & e_3 & \dots & 0 & 0 & 0 & J_1 & \dots & 0 & 0 \\ \vdots & \vdots & \ddots & \vdots & \vdots & \vdots & \vdots & \ddots & \vdots & \vdots \\ 0 & 0 & \dots & e_3 & 0 & 0 & 0 & \dots & -I & 0 \\ 0 & 0 & \dots & 0 & e_3 & 0 & 0 & \dots & J_{n-1} & -I \\ 0 & 0 & \dots & 0 & 0 & 0 & 0 & \dots & 0 & I \end{bmatrix}$$

is full rank. By row reduction, it is equivalent that

$$[(J_{n-1} \dots J_1) e_3 \quad \dots \quad J_{n-1} e_3 \quad e_3] \quad (10)$$

is full rank. The matrix (10) is the manipulator Jacobian, so  $(u, x)$  is regular if and only if it defines a non-singular configuration of the kinematic chain. Non-singular configurations are exactly those satisfying  $u(i) \notin \{k\pi: k \in \mathbb{Z}\}$  for some  $i \in \{1, \dots, n-1\}$  (e.g., see [45]). ■

**Lemma 5:** A point  $\phi(a)$  is regular with respect to (2) if and only if  $a \in \mathcal{A}$ .

*Proof:* We will prove the converse, that  $(u, x) = \phi(a)$  is not regular if and only if  $a \in \mathcal{S} = \mathbb{R}^3 \setminus \mathcal{A}$ . By Lemma 4, it is equivalent to show that  $u(i) \in \{k\pi: k \in \mathbb{Z}\}$  for all  $i \in \{0, \dots, n-1\}$  if and only if  $a \in \mathcal{S}$ .

First, let  $a \in \mathcal{S}$  and take  $(u, x) = \phi(a)$ . We have

$$\begin{aligned} u(0) &= -a_3 && \text{(by Lemma 3)} \\ &\in \{k\pi: k \in \mathbb{Z}\} && \text{(by definition of } \mathcal{S}\text{).} \end{aligned}$$

For some  $i \in \{1, \dots, n-1\}$ , assume  $u(j) \in \{k\pi: k \in \mathbb{Z}\}$  for all  $j \in \{0, \dots, i-1\}$ . From (5), it must also be true that

$x_1(i+1) = m(n-1)^{-1}$  and  $x_2(i+1) = 0$  for some  $m \in \mathbb{Z}$ . By Lemma 3 and the definition of  $\mathcal{S}$ , we conclude that

$$u(i) = a_2 m(n-1)^{-1} - a_3 = (km - l)\pi$$

for some  $k, l \in \mathbb{Z}$ , hence that  $u(i) \in \{k\pi : k \in \mathbb{Z}\}$ . Our result proceeds by induction.

Now, let  $a \in \mathbb{R}^3$ , take  $(u, x) = \phi(a)$ , and assume  $u(i) \in \{k\pi : k \in \mathbb{Z}\}$  for all  $i \in \{0, \dots, n-1\}$ , so  $u(0) = m_0\pi$  and  $u(1) = m_1\pi$  for some  $m_0, m_1 \in \mathbb{Z}$ . From (5), we compute

$$x(1) = \begin{bmatrix} 0 \\ 0 \\ m_0\pi \end{bmatrix} \quad \text{and} \quad x(2) = \begin{bmatrix} 0 \\ (n-1)^{-1} \cos(m_0\pi) \\ (m_0 + m_1)\pi \end{bmatrix}.$$

By Lemma 3, we have

$$\begin{aligned} m_0\pi &= u(0) = -a_3 \\ m_1\pi &= u(1) = a_2(n-1)^{-1} \cos(m_0\pi) - a_3. \end{aligned}$$

Solving, we find that

$$\begin{aligned} a_2 &= \pm(m_1 - m_0)(n-1)\pi \\ a_3 &= -m_0\pi, \end{aligned}$$

hence that  $a \in \mathcal{S}$ .  $\blacksquare$

We are now ready to prove our main result.

*Lemma 6:* The map  $\phi: \mathcal{A} \rightarrow \mathcal{C}$  is a homeomorphism.

*Proof:* First, we will show that  $\phi$  is a continuous bijection. By construction,  $\phi(a)$  satisfies (3)-(4) for the choice of costate  $\rho(a)$ , for any  $a \in \mathbb{R}^3$ . By Lemma 5,  $\phi(a)$  is regular if and only if  $a \in \mathcal{A} \subset \mathbb{R}^3$ . As a consequence,  $\phi$  is both well-defined and onto. The continuity of  $\phi$  then follows immediately from (5). Finally, recall that if  $(u, x) \in \mathcal{C}$  is regular, then the costate  $p$  satisfying (3)-(4) is unique [38]. In particular,  $p(0) = a$  is unique, so  $\phi$  is one-to-one.

By Lemma 2 (Appendix I), it remains only to show that  $\phi$  is a local homeomorphism. Fix  $a \in \mathcal{A}$ . Since  $\mathcal{A}$  is locally compact, then  $a$  has a compact neighborhood  $\mathcal{U} \subset \mathcal{A}$  on which the restriction  $\phi|_{\mathcal{U}}: \mathcal{U} \rightarrow \phi(\mathcal{U})$  is also a continuous bijection. Since  $\mathbb{R}^n \times \mathbb{R}^{3(n+1)}$  is Hausdorff under the standard topology, then the image  $\phi(\mathcal{U}) \subset \mathcal{C} \subset \mathbb{R}^n \times \mathbb{R}^{3(n+1)}$  is Hausdorff under the subspace topology. We have established that  $\phi|_{\mathcal{U}}$  is a continuous bijection between compact  $\mathcal{U}$  and Hausdorff  $\phi(\mathcal{U})$ , so  $\phi|_{\mathcal{U}}$  is a homeomorphism [46, Theorem 5.6, p167]. Our choice of  $a$  was arbitrary, so  $\phi$  is a local homeomorphism, as desired.  $\blacksquare$

### APPENDIX III

#### PROOF THAT DISCRETEISSTABLE IS CORRECT

Our main result in this section is a proof of Theorem 4, which establishes correctness of the algorithm DISCRETEISSTABLE (Fig. 2) in Section II-C. We will first prove one supporting lemma.

*Lemma 7:* Pick  $a \in \mathbb{R}^3$  and let  $(u, x) = \phi(a)$ . If for some  $i \in \{0, \dots, n-2\}$  there exist  $m_i, m_{i+1} \in \mathbb{Z}$  such that  $u(i) = m_i\pi$  and  $u(i+1) = m_{i+1}\pi$ , then  $a \in \mathcal{S}$ .

*Proof:* From (5) and Lemma 3, we compute

$$\begin{aligned} m_i\pi &= u(i-1) - a_1 r_i \sin x_3(i) + a_2 r_i \cos x_3(i) \\ m_{i+1}\pi &= m_i\pi + \cos m_i\pi (-a_1 r_i \sin x_3(i) + a_2 r_i \cos x_3(i)). \end{aligned}$$

Solving, we find that

$$u(i-1) = (m_i \pm (m_i - m_{i+1}))\pi = m_{i-1}\pi$$

for some  $m_{i-1} \in \mathbb{Z}$ . By repeating this process, we would find that  $u(0) = m_0\pi$  and  $u(1) = m_1\pi$  for some  $m_0, m_1 \in \mathbb{Z}$ . An argument identical to the one found in our proof of Lemma 5 (Appendix II) then establishes that  $a \in \mathcal{S}$ .  $\blacksquare$

We are now ready to prove our main result, that  $a \in \mathcal{A}_{\text{stable}}$  if and only if DISCRETEISSTABLE( $a$ ) returns TRUE.

*Proof:* [Proof of Theorem 4] Assume DISCRETEISSTABLE( $a$ ) returns TRUE. Let  $v_j(z)$  be the cost-to-go from  $\delta x(j) = z$  in (8), for  $j \in \{0, \dots, n-1\}$ . We have

$$v_{n-4}(z) = \min_y \left\{ \frac{1}{2} y^T M y : A y = B z \right\}, \quad (11)$$

where  $A, B$ , and  $M$  are as defined in Fig. 2. The matrix  $A$  loses rank if and only if  $u(n-3) = k\pi$  and  $u(n-2) = l\pi$  for some  $k, l \in \mathbb{Z}$ , which by Lemma 7 contradicts our assumption that  $a \in \mathcal{A}$ , so  $A$  is full rank. Therefore, we can rewrite (11) as the quadratic form

$$v_{n-4}(z) = \min_y \left\{ \frac{1}{2} (A^\dagger B z + N y)^T M (A^\dagger B z + N y) \right\}.$$

Since  $N^T M N > 0$  by assumption, we conclude that

$$v_{n-4}(z) = z^T P_{n-4} z,$$

where the minimum is achieved by  $y = -K A^\dagger B z$ . With a standard dynamic programming argument, we have

$$\begin{aligned} v_i(z) &= \min_{\delta u(i)} \left\{ \frac{1}{2} (z^T Q_i z + \delta u(i)^2) \right. \\ &\quad \left. + v_{i+1}(J_i z + e_3 \delta u(i)) \right\} \end{aligned} \quad (12)$$

for  $i \in \{n-5, \dots, 0\}$ . If

$$v_{i+1}(z) = z^T P_{i+1} z,$$

then since

$$s_{i+1} = 1 + e_3^T P_{i+1} e_3 > 0$$

by assumption, we conclude that

$$\begin{aligned} v_i(z) &= z^T (Q_i + J_i^T (P_{i+1} - P_{i+1} e_3 s_{i+1}^{-1} e_3^T P_{i+1}) J_i) z \\ &= z^T P_i z, \end{aligned}$$

where the minimum is achieved by

$$\delta u(i) = -s_{i+1}^{-1} e_3^T P_{i+1} J_i^T z.$$

In particular,  $v_0(z) = z^T P_0 z$  and  $\delta u(0) = -s_1^{-1} e_3^T P_1 J_0^T z$ . Since we are given  $\delta x(0) = 0$ , we find that  $\delta u(0) = 0$ , hence that  $\delta x(1) = 0$  as well. Repeating this process, we see that (8) has unique solution  $(\delta u, \delta x) = (0, 0)$ , so  $a \in \mathcal{A}_{\text{stable}}$ .

Now, assume DISCRETEISSTABLE( $a$ ) returns FALSE. If  $N^T M N \not> 0$ , then (11) is either unbounded below or admits multiple solutions for  $y$ , both of which imply that  $a \notin \mathcal{A}_{\text{stable}}$ . If  $1 + e_3^T P_{i+1} e_3 \not> 0$  for some  $i \in \{n-5, \dots, 0\}$ , then (12) is either unbounded below or admits multiple solutions for  $\delta u(i)$ , both of which again imply that  $a \notin \mathcal{A}_{\text{stable}}$ . These are the only two possibilities, so we have our result.  $\blacksquare$

## ACKNOWLEDGMENTS

Thanks to S. Hutchinson for helpful discussions. This material is based upon work supported by the National Science Foundation under CPS-0931871 and CMMI-0956362.

## REFERENCES

- [1] F. Lamiraux and L. E. Kavraki, "Planning paths for elastic objects under manipulation constraints," *International Journal of Robotics Research*, vol. 20, no. 3, pp. 188–208, 2001.
- [2] M. Moll and L. E. Kavraki, "Path planning for deformable linear objects," *IEEE Trans. Robot.*, vol. 22, no. 4, pp. 625–636, Aug. 2006.
- [3] J. E. Hopcroft, J. K. Kearney, and D. B. Krafft, "A case study of flexible object manipulation," *The International Journal of Robotics Research*, vol. 10, no. 1, pp. 41–50, 1991.
- [4] J. Takamatsu, T. Morita, K. Ogawara, H. Kimura, and K. Ikeuchi, "Representation for knot-tying tasks," *IEEE Trans. Robot.*, vol. 22, no. 1, pp. 65–78, Feb. 2006.
- [5] H. Wakamatsu, E. Arai, and S. Hirai, "Knotting/un-knotting manipulation of deformable linear objects," *The International Journal of Robotics Research*, vol. 25, no. 4, pp. 371–395, 2006.
- [6] M. Saha and P. Ito, "Manipulation planning for deformable linear objects," *IEEE Trans. Robot.*, vol. 23, no. 6, pp. 1141–1150, Dec. 2007.
- [7] M. Bell and D. Balkcom, "Knot tying with single piece fixtures," in *Int. Conf. Rob. Aut.*, May 2008, pp. 379–384.
- [8] J. van den Berg, S. Miller, D. Duckworth, H. Hu, A. Wan, X.-Y. Fu, K. Goldberg, and P. Abbeel, "Superhuman performance of surgical tasks by robots using iterative learning from human-guided demonstrations," in *Int. Conf. Rob. Aut.*, May 2010, pp. 2074–2081.
- [9] H. Inoue and H. Inaba, "Hand-eye coordination in rope handling," in *Robotics Research: The First International Symposium*, 1985, pp. 163–174.
- [10] M. Bell, "Flexible object manipulation," Ph.D. dissertation, Dartmouth College, Hanover, NH, Feb. 2010.
- [11] J. van den Berg, S. Miller, K. Goldberg, and P. Abbeel, "Gravity-based robotic cloth folding," in *Algorithmic Foundations of Robotics IX*, ser. Springer Tracts in Advanced Robotics, D. Hsu, V. Isler, J.-C. Latombe, and M. Lin, Eds. Springer Berlin / Heidelberg, 2011, vol. 68, pp. 409–424.
- [12] Y. Yamakawa, A. Namiki, and M. Ishikawa, "Motion planning for dynamic folding of a cloth with two high-speed robot hands and two high-speed sliders," in *Int. Conf. Rob. Aut.*, May 2011, pp. 5486–5491.
- [13] D. J. Balkcom and M. T. Mason, "Robotic origami folding," *The International Journal of Robotics Research*, vol. 27, no. 5, pp. 613–627, 5 2008.
- [14] Y. Asano, H. Wakamatsu, E. Morinaga, E. Arai, and S. Hirai, "Deformation path planning for manipulation of flexible circuit boards," in *IEEE/RSJ Int. Conf. Int. Rob. Sys.*, Oct. 2010, pp. 5386–5391.
- [15] R. Jansen, K. Hauser, N. Chentanez, F. van der Stappen, and K. Goldberg, "Surgical retraction of non-uniform deformable layers of tissue: 2d robot grasping and path planning," in *IEEE/RSJ Int. Conf. Int. Rob. Sys.*, Oct. 2009, pp. 4092–4097.
- [16] Q. Lin, J. Burdick, and E. Rimon, "A stiffness-based quality measure for compliant grasps and fixtures," *IEEE Trans. Robot. Autom.*, vol. 16, no. 6, pp. 675–688, Dec. 2000.
- [17] J.-S. Cheong, K. Goldberg, M. Overmars, and A. van der Stappen, "Fixturing hinged polygons," in *Int. Conf. Rob. Aut.*, vol. 1, 2002, pp. 876–881.
- [18] K. Gopalakrishnan and K. Goldberg, "D-space and deform closure grasps of deformable parts," *International Journal of Robotics Research*, vol. 24, no. 11, pp. 899–910, Nov. 2005.
- [19] N. M. Amato and G. Song, "Using motion planning to study protein folding pathways," *Journal of Computational Biology*, vol. 9, no. 2, pp. 149–168, 2002.
- [20] M. S. Apaydin, D. L. Brutlag, C. Guestrin, D. Hsu, J.-C. Latombe, and C. Varma, "Stochastic roadmap simulation: An efficient representation and algorithm for analyzing molecular motion," *Journal of Computational Biology*, vol. 10, no. 3–4, pp. 257–281, 2003.
- [21] J. Cortés, T. Siméon, M. Remaud-Siméon, and V. Tran, "Geometric algorithms for the conformational analysis of long protein loops," *Journal of Computational Chemistry*, vol. 25, no. 7, pp. 956–967, 2004.
- [22] M. L. Teodoro, G. N. Phillips, and L. E. Kavraki, "Understanding protein flexibility through dimensionality reduction," *Journal of Computational Biology*, vol. 10, no. 3–4, pp. 617–634, 07 2004.
- [23] H. Tanner, "Mobile manipulation of flexible objects under deformation constraints," *IEEE Trans. Robot.*, vol. 22, no. 1, pp. 179–184, Feb. 2006.
- [24] G. S. Chirikjian and J. W. Burdick, "The kinematics of hyper-redundant robot locomotion," *IEEE Trans. Robot. Autom.*, vol. 11, no. 6, pp. 781–793, Dec. 1995.
- [25] M. W. Hannan and I. D. Walker, "Kinematics and the implementation of an elephant's trunk manipulator and other continuum style robots," *Journal of Robotic Systems*, vol. 20, no. 2, pp. 45–63, 2003.
- [26] B. A. Jones and I. D. Walker, "Kinematics for multisection continuum robots," *IEEE Trans. Robot.*, vol. 22, no. 1, pp. 43–55, Feb. 2006.
- [27] D. B. Camarillo, C. F. Milne, C. R. Carlson, M. R. Zinn, and J. K. Salisbury, "Mechanics modeling of tendon-driven continuum manipulators," *IEEE Trans. Robot.*, vol. 24, no. 6, pp. 1262–1273, Dec. 2008.
- [28] D. C. Rucker, R. J. Webster, G. S. Chirikjian, and N. J. Cowan, "Equilibrium conformations of concentric-tube continuum robots," *The International Journal of Robotics Research*, vol. 29, no. 10, pp. 1263–1280, 09 2010.
- [29] R. J. Webster and B. A. Jones, "Design and kinematic modeling of constant curvature continuum robots: A review," *The International Journal of Robotics Research*, vol. 29, no. 13, pp. 1661–1683, 11 2010.
- [30] Y. Nakamura, *Advanced robotics: redundancy and optimization*. Reading, Mass.: Addison-Wesley Pub. Co., 1991.
- [31] A. Shkolnik and R. Tedrake, "Path planning in 1000+ dimensions using a task-space voronoi bias," in *Int. Conf. Rob. Aut.*, Kobe, Japan, May 2009, pp. 2061–2067.
- [32] M. Behnisch, R. Haschke, and M. Gienger, "Task space motion planning using reactive control," in *IEEE/RSJ Int. Conf. Int. Rob. Sys.*, Oct. 2010, pp. 5934–5940.
- [33] G. Chirikjian and J. Burdick, "A modal approach to hyper-redundant manipulator kinematics," *IEEE Trans. Robot. Autom.*, vol. 10, no. 3, pp. 343–354, Jun. 1994.
- [34] A. De Luca and G. Oriolo, "Nonholonomic behavior in redundant robots under kinematic control," *IEEE Trans. Robot. Autom.*, vol. 13, no. 5, pp. 776–782, Oct. 1997.
- [35] A. De Luca, R. Mattone, and G. Oriolo, "Steering a class of redundant mechanisms through end-effector generalized forces," *IEEE Trans. Robot. Autom.*, vol. 14, no. 2, pp. 329–335, Apr. 1998.
- [36] O. Khatib, "A unified approach for motion and force control of robot manipulators: The operational space formulation," *IEEE J. of Rob. and Aut.*, vol. RA-3, no. 1, 1987.
- [37] A. E. Bryson and Y.-C. Ho, *Applied Optimal Control*. Hemisphere Publishing, 1975.
- [38] D. G. Luenberger and Y. Ye, *Linear and nonlinear programming*, 3rd ed., ser. International series in operations research & management science. New York: Springer, 2007, vol. 116.
- [39] J.-C. Latombe, *Robot Motion Planning*. Boston, MA: Kluwer Academic Publishers, 1991.
- [40] H. Choset, K. Lynch, S. Hutchinson, G. Kanto, W. Burgard, L. Kavraki, and S. Thrun, *Principles of Robot Motion: Theory, Algorithms, and Implementations*. MIT Press, 2005.
- [41] S. M. LaValle, *Planning algorithms*. New York, NY: Cambridge University Press, 2006.
- [42] L. E. Kavraki, P. Svetkska, J.-C. Latombe, and M. Overmars, "Probabilistic roadmaps for path planning in high-dimensional configuration spaces," *IEEE Trans. Robot. Autom.*, vol. 12, no. 4, pp. 566–580, 1996.
- [43] J. M. Lee, *Introduction to smooth manifolds*. New York: Springer, 2003, vol. 218.
- [44] J. Lee, *Introduction to topological manifolds*, ser. Graduate texts in mathematics. Springer, 2000.
- [45] J. Trinkle and R. Milgram, "Complete path planning for closed kinematic chains with spherical joints," *Int. J. Rob. Res.*, vol. 21, no. 9, pp. 773–789, 2002.
- [46] J. R. Munkres, *Topology; a first course*. Englewood Cliffs, N.J.: Prentice-Hall, 1975.